

# 2-inch Diameter (100) $\beta$ -Ga<sub>2</sub>O<sub>3</sub> Crystal Growth by the Vertical Bridgman Technique in a Resistance Heating Furnace in Ambient Air

\*K. Hoshikawa<sup>1</sup>, T. Kobayashi<sup>1</sup>, Y. Matsuki<sup>1</sup>, E. Ohba<sup>2</sup>, T. Kobayashi<sup>2</sup>

Faculty of Engineering, Shinshu University, Nagano, Japan<sup>1</sup>

Fujikoshi Machinery Corp., Nagano, Japan<sup>2</sup>

\*E-mail: [khoshi1@shinshu-u.ac.jp](mailto:khoshi1@shinshu-u.ac.jp)

## Abstract

A resistance heating vertical Bridgman (VB) furnace able to maintain high temperatures up to 1830°C in ambient air was developed to suppress weight loss of both the crucible and raw material Ga<sub>2</sub>O<sub>3</sub>. Large-size 50 mm diameter  $\beta$ -Ga<sub>2</sub>O<sub>3</sub> crystals with a growth orientation perpendicular to (100) plane were grown by the VB growth process in platinum-rhodium alloy crucibles using this furnace. The total weight loss during a VB growth run is very small, amounting to less than 1% of the total weight of the platinum-rhodium alloy crucible and the Ga<sub>2</sub>O<sub>3</sub> raw material.

Key words;

A1. Crystallites

A1. Solidification

A2. Bridgman technique

A2. Single crystal growth

B1. Oxides

B2.  $\beta$ -Ga<sub>2</sub>O<sub>3</sub> single crystal

## 1. Introduction

$\beta$ -Ga<sub>2</sub>O<sub>3</sub> is an oxide semiconductor with a wide band gap of 4.7-4.9 eV [1, 2]. Because  $\beta$ -Ga<sub>2</sub>O<sub>3</sub> is a wide band gap semiconductor suitable for next-generation power devices due to its high breakdown voltage and high current density, the research for growth techniques that produce larger and better quality  $\beta$ -Ga<sub>2</sub>O<sub>3</sub> crystals has intensified recently.

[3-6].

$\beta$ -Ga<sub>2</sub>O<sub>3</sub> bulk crystals have until now been grown by optical floating-zone (OFZ) [7-9], Czochralski (CZ) [10-12] and edge-defined, film-fed growth (EFG) [13, 14] methods. With the OFZ method,  $\beta$ -Ga<sub>2</sub>O<sub>3</sub> crystals can generally be grown in ambient air because the method requires no crucible. Consequently, this method has been widely used to prepare experimental samples with relative ease. However, crystals grown using OFZ are dimensionally limited due to the limited size of the light spot. Also, defects will always be present at high density as the melt zone occupies a small volume and may not cover the whole crystal diameter.  $\beta$ -Ga<sub>2</sub>O<sub>3</sub> crystals produced by the CZ and the EFG methods have been grown from melts in iridium crucibles, and  $\beta$ -Ga<sub>2</sub>O<sub>3</sub> substrates grown by the EFG method have recently become commercially available. However, these two methods have some technical problems, such as the necessity of atmosphere control due to the use of an iridium crucible. An oxidizing atmosphere is desirable for  $\beta$ -Ga<sub>2</sub>O<sub>3</sub> crystal growth because  $\beta$ -Ga<sub>2</sub>O<sub>3</sub> is an oxide that undergoes reductive decomposition ( $\text{Ga}_2\text{O}_3 \rightarrow 2\text{Ga} + 3/2\text{O}_2$ ) at high temperatures due to a deficiency of oxygen [10-12, 15, 16]. This problem links to the fact that iridium crucibles are not useful in atmospheres with more than a few percent of oxygen partial pressure at the high temperature required to melt  $\beta$ -Ga<sub>2</sub>O<sub>3</sub> because iridium will easily oxidize and evaporate under those conditions [12, 17]. This presents an atmosphere control problem for  $\beta$ -Ga<sub>2</sub>O<sub>3</sub> crystal growth in an iridium crucible. These considerations indicate that the suppression of both Ir oxidization and Ga<sub>2</sub>O<sub>3</sub> decomposition are in conflict, due to the need for high temperature during the growth of  $\beta$ -Ga<sub>2</sub>O<sub>3</sub> by the CZ and the EFG methods, and the fact that Ir crucibles must be used. It has been increasingly acknowledged that the high temperature chemical stability of both the molten  $\beta$ -Ga<sub>2</sub>O<sub>3</sub> and the Ir crucible during growth processes are significant challenges in the growth of large-sized and high quality  $\beta$ -Ga<sub>2</sub>O<sub>3</sub> crystals.

To solve this problem, we have proposed a new approach in which  $\beta$ -Ga<sub>2</sub>O<sub>3</sub> crystals are grown in ambient air, as suppressing Ga<sub>2</sub>O<sub>3</sub> decomposition is the most important issue in the growth of large and high quality  $\beta$ -Ga<sub>2</sub>O<sub>3</sub> crystals. We have studied the growth of  $\beta$ -Ga<sub>2</sub>O<sub>3</sub> single crystals by the vertical Bridgman (VB) method [18-20], in which diameter control was unnecessary and the crystals could be grown in a very low temperature gradient. As a result, we could use platinum-rhodium alloy crucibles, the melting temperature of which was approximately 50°C higher than that of  $\beta$ -Ga<sub>2</sub>O<sub>3</sub>, and the crucibles could be useful in oxidizing atmospheres, including ambient air, in which an iridium crucible was far from adequate [21].

We reported in our previous papers [21, 22] the successful growth of  $\beta$ -Ga<sub>2</sub>O<sub>3</sub> single crystals about 25 mm in diameter by the VB method, using platinum-rhodium alloy

crucibles in ambient air. In our previous papers [21, 22], we had used the radio frequency heating technique to realize high temperatures above the melting temperature of  $\beta$ -Ga<sub>2</sub>O<sub>3</sub> in the VB furnace. We concluded, however, that growing large high quality  $\beta$ -Ga<sub>2</sub>O<sub>3</sub> crystals had proved a challenge due to the difficulty of producing a uniform temperature distribution in the large furnace zone by radio frequency heating. To solve this, we have worked to construct a resistance heating furnace with a temperature above 1830°C in ambient air, and to grow  $\beta$ -Ga<sub>2</sub>O<sub>3</sub> crystals by the VB technique using platinum-rhodium alloy crucibles. Using this furnace, we have grown  $\beta$ -Ga<sub>2</sub>O<sub>3</sub> crystals with a diameter of 50 mm.

This paper briefly introduces the newly developed resistance heating furnace and presents the VB growth processes and the results of the endeavor to produce  $\beta$ -Ga<sub>2</sub>O<sub>3</sub> single crystals with a growth orientation perpendicular to (100) plane using the developed furnace.

## 2. Experimental

The VB furnace developed for our growth of  $\beta$ -Ga<sub>2</sub>O<sub>3</sub> crystals is shown in Fig. 1. Figure 1(a) is a photograph and Fig. 1(b) is a schematic of the resistance heating furnace. The heaters were mainly made of molybdenum silicide, and heat shields were constructed using a heat-resistant board comprising mainly aluminum oxide. The furnace tube and the crucible support were constructed from zirconia oxide and aluminum oxide. B-type thermocouples (B-TC) were used to measure the temperature at the crucible bottom as the temperature there was less than 1800°C. The crucibles were made of the platinum-rhodium alloy previously reported in our papers [21, 22]. The visual image in Fig. 1(a) and the inner furnace structure shown in Fig. 1(b) are not very different from a conventional resistance heating electric furnace. Several new approaches, however, were attempted in relation to the materials and the detailed structures of the heater and the heat shield, especially in the electric and thermal insulator used between heater electrode and heat shield. This is because it was not only very challenging to realize the high temperature of 1830°C in the furnace zone, but also to achieve the VB growth of  $\beta$ -Ga<sub>2</sub>O<sub>3</sub> in ambient air. The temperature distribution of the furnace shown in Fig.1 is shown in Fig. 2 as an example.

The VB growth processes were as follows. The crucible, charged with a seed crystal and a sintered body of Ga<sub>2</sub>O<sub>3</sub> raw material, was elevated to melt all of the raw material body and part of the seed crystal during the VB seeding process (shown as schematic (a) in Fig. 2). Then the crucible was lowered at a constant rate from 1 to 5 mm/hour during the VB

growth process, as shown in schematics (a) and (b) in Fig. 2. The crucible was rotated at a constant rate of 3 rpm during seeding and growth processes. We measured temperatures at two positions near the seed portion at the crucible bottom by using a B-TC connected to the crucible periphery by fusion splicing, as shown in schematics (a) and (b) in Fig. 2. The crystals grown by the VB process in the platinum-rhodium alloy crucible were released from the crucibles by destructively peeling it from the crystal periphery [21].

### 3. Results and discussion

#### 3.1 Growth of single crystal with growth orientation perpendicular to (100) plane

Figure 3 shows the logger data during the melting, seeding, and initial growth processes of a  $\beta$ -Ga<sub>2</sub>O<sub>3</sub> crystal. The variation in TCh shows the temperature change near the heater as measured by the platinum-rhodium (20-40%) thermocouples. The variation in CP shows the crucible position change, and the variations TC1 and TC2 show the temperature changes measured by the B-TC of TC1 and TC2 shown in Fig. 2. The variations of TCh, TC1 and TC2 during the melting process are related to the heater power being artificially controlled. The variations of TC1 and TC2 in the seeding and growth processes are mainly related to the crucible position (CP) change, but the simultaneous changes of TCh, TC1 and TC2 at positions P1 and P2 are related to the heater power control. The abrupt change of TC1 at position M1 may be related to a downward flow of molten raw material melted at the upper part of the crucible, where the temperature was higher than that at the crucible bottom.

A photograph of a seed portion separately cut by a slicer is shown in Fig. 4. Arrow A shows the seeding interface position, at about 27 mm from the bottom of the seed, because there were no gaps between the crystal and the crucible inner wall above the interface, but there were some gaps below the interface. Arrow B shows the boundary of two seed crystals with a growth orientation perpendicular to (100) plane. These were used because we did not have crystals long enough to make a seed. TC1 and TC2 in Fig. 4 show two B-TC positions connected by fusion splicing; data from these TCs were recorded during all growth processes.

A photograph in Fig. 5(a) shows a crystal ingot that began polycrystalline growth in half of its body after single-crystal growth at conical portion and half of the body following (100) single crystal seeding. A photograph of a cross-section at the center portion cut perpendicular to the portion enclosed by a dashed line in Fig. 5(a) is shown in Fig. 5(b). In Fig. 5(b), straight boundary lines nearly perpendicular to the growth direction show

(100) faceted growth traces. Some polycrystalline growth seems to be started at portions of the outer periphery of the faceted growth shown by the straight boundary lines. The slight tilting of the lines must correspond to the seed crystal tilting from the growth orientation perpendicular to (100) plane. It was found in the present experiment and from consideration of the results of (100) growth that maintaining (100) faceted growth during crystallization of all the melt, especially the final stage in the VB growth process, is an essential condition for the successful growth of a single crystal. We concluded from the above considerations that to ensure the growth of a 100% single crystal, a more homogeneous temperature distribution must be realized in the radial direction perpendicular to the (100) faceted growth plane [21], and the seed crystals used had to be precisely (100).

We measured and recorded the temperature difference  $\Delta T$  between TC1 and TC2 during the growth processes. The representative two characteristics of the  $\Delta T$  vs. these TCs moving distance from the positions at the growth start are shown in Fig. 6. Characteristic (a) in Fig. 6 shows the  $\Delta T$  variation in the growth of the crystal shown in Fig. 5 and characteristic (b) shows the  $\Delta T$  variation in the growth of another crystal, which was grown under improved control, specifically, improved temperature distribution and decreased crucible lowering rate. The temperature difference  $\Delta T$  changed from 3 to 9°C during a 90 mm move of TC1 and TC2 as shown by characteristic (a) in Fig. 6. On the other hand,  $\Delta T$  changed from 0.8 to 8°C as shown by characteristic (b) in Fig. 6. Applying the temperature conditions shown by characteristic (b) in Fig. 6, we succeeded in growing  $\beta$ -Ga<sub>2</sub>O<sub>3</sub> single-crystals with a growth orientation perpendicular to (100) plane and 50 mm in diameter by 50 mm long, as shown in Fig. 7. A crucible lowering rate of 1 mm/h was tried during the growth of the crystal shown in Fig. 7, while the higher rate of 2 mm/h had been applied during the growth of the crystal shown in Fig. 5.

The photographs in Figs. 7(a), (b) and (c) respectively show top, side and bottom views of the single crystal grown. In the top view of Fig. 7(a), a circle mirror plane observed at the upper side is a (100) plane where the seed portion was easily removed due to cleavage failure. Two crystal habit lines formed by (100) and (001) cleavage planes are clearly observed at the surface of the conical periphery. In the side view of Fig. 7(b), it is noteworthy that the as-grown crystal surface after removing the platinum-rhodium alloy crucible was very smooth and shiny, as already reported in the previous papers [21]. In the bottom view of Fig. 7(c), a crystal habit of straight lines with [010] direction was clearly observed at the bottom surface and some polycrystalline regions were generated during the final growth stage at the terminal edge of the crystal's periphery. We think that in VB growth the perfect single-crystal growth of  $\beta$ -Ga<sub>2</sub>O<sub>3</sub> may be difficult to realize, as

with various other kinds of crystals because of a fundamental problem with the 100% solidification of a melt in a crucible.

Photographs of as-sliced wafers and a mirror-polished wafer with a (100) plane are shown in Fig. 8. The dark yellow color of the wafers in Fig. 8 might be caused by rhodium contamination from the platinum-rhodium alloy crucible, as suggested by the impurity analysis results in section 3.3.

### **3.2 Weight loss of crucible and raw material Ga<sub>2</sub>O<sub>3</sub>**

The total weight losses from the Ga<sub>2</sub>O<sub>3</sub> raw material and the crucible during the growth process in three serial runs are shown in Table 1. In Table 1, the total weight of raw material and crucible is a weight of the crucible charged with Ga<sub>2</sub>O<sub>3</sub> raw material including a seed crystal, which was measured in the preparation process of the growth run. The retention time at more than 1770°C refers to the total time when the whole crucible was kept in the high temperature zone at 1770°C to 1820°C during the seeding and growth processes, as explained in Fig. 2.

We also investigated the weight loss of the crucible alone by an experiment in which we used an empty 51.0 g platinum-rhodium alloy crucible, identical to that used in the crystal growth runs shown in Table 1. The weight loss was only 0.227 g when an empty crucible was kept for 97 hours in the high temperature zone at 1770 to 1820°C in a simulation of the growth process of run number 1 in Table 1. This indicated that the total weight loss in Table 1 was mainly due to weight losses of Ga<sub>2</sub>O<sub>3</sub> raw material in the melting process and molten Ga<sub>2</sub>O<sub>3</sub> in seeding and growth processes. The total weight loss might depend on the time spent by the crucible in the high temperature zone, but a clear dependency is not found in Table 1, which also showed no dependency between the total weight loss and the total weight of raw material and crucible.

The weight losses of crucible material and raw material Ga<sub>2</sub>O<sub>3</sub> are very important contributing factors in the successful growth of β-Ga<sub>2</sub>O<sub>3</sub> crystals because the crucibles are easily oxidized and evaporated under a certain oxygen partial pressure, and in the opposite direction, the raw material Ga<sub>2</sub>O<sub>3</sub> is easily decomposed and evaporated under a lower oxygen partial pressure. We could conclude that both crucible weight loss and also raw material weight loss were very small in our present VB β-Ga<sub>2</sub>O<sub>3</sub> crystal growth technique by using a platinum-rhodium alloy crucible in ambient air. It was stressed that the mean total weight loss in three growth runs was only 3.3 g from a 501 g total weight of raw material and crucible during a 93-hour retention at 1770 to 1820°C.

### **3.3 Chemical analysis of VB grown β-Ga<sub>2</sub>O<sub>3</sub> (100) crystals**

Impurity analysis results for VB  $\beta$ -Ga<sub>2</sub>O<sub>3</sub> crystals grown using a platinum-rhodium alloy crucible in ambient air are shown in Table 2. The impurity analysis was conducted by GDMS using VG Elemental VG9000 (Toray Research Center Inc.) [21]. In Table 2,  $g=0.5$  and  $g=0.9$  show the solidification fraction values of sample positions cut from a crystal ingot. The purity of raw material used was five nines (99.999%), and the concentration of each undesired element found was less than 1.0 ppm by weight (wt.ppm), according to data from Yamanaka Hutech Corp. The impurities Si, Fe, Zr and Rh, the concentrations of which exceeded 1.0 wt.ppm, were understood to have become contaminants during the growth process. The Si, Fe and Zr might result from contamination by furnace materials, while the 30 wt.ppm Rh must be contamination from the platinum-rhodium alloy crucibles. These will be subjects for a future investigation of the influence of such a concentration of Rh on semiconductor characteristics, and we must also suppress the Rh contamination by using improved crucible materials and/or improved growth processes. The concentrations of most of the impurity elements except Al and Pt increased with increasing solidification fraction from 0.5 to 0.9 in Table 2. Thus we conclude that this concentration increase may relate to the segregation of each impurity present in the molten raw material Ga<sub>2</sub>O<sub>3</sub>. We attempted to examine the Hall effect at room temperature for the impurity analysis samples prepared from the near portion with  $g=0.5$  by using Toyo-Technica ResiTest8400, but the measurement could not be performed due to measurement limit with more than 10ohm-cm of resistivity. However, the voltage-current measurement method with indium-gallium electrode showed high resistivity characteristic more than  $10^7$  ohm-cm at room temperature.

The crystallinity evaluation of VB grown (100) wafers has been inadequate because the required procedures for slicing and polishing (100) wafers were not available due to (100) cleavage in the slicing process and micro-cracks and micro-cleavage on the (100) plane in the lapping and polishing processes. As a result, the crystallinity evaluation of bulk crystal, i.e. characteristics determined by full-width at half-maximum (FWHM), X-ray topography and etching for dislocation pits, is an issue for future study.

#### **4. Summary and conclusions**

- (1) We developed a resistance heating VB furnace that could maintain temperatures up to 1830°C in ambient air.
- (2)  $\beta$ -Ga<sub>2</sub>O<sub>3</sub> single crystals 50 mm in diameter, 50 mm long, and a growth orientation perpendicular to (100) plane have been grown in platinum-rhodium alloy crucibles using the furnace developed.

- (3) The weight losses during a growth run of the VB process were very small, less than 1% of the total weight of the platinum-rhodium alloy crucible and the Ga<sub>2</sub>O<sub>3</sub> raw material, and most of them proved to be weight loss of Ga<sub>2</sub>O<sub>3</sub>.
- (4) The unintentionally doped VB-grown β-Ga<sub>2</sub>O<sub>3</sub> crystals contained significant rhodium impurity, with 30 wt.ppm originating in the platinum-rhodium alloy crucible.

We concluded in our present study that the resistance heating VB furnace developed could maintain a high temperature up to 1830°C in ambient air and made possible the successful growth of large β-Ga<sub>2</sub>O<sub>3</sub> crystals with very small weight loss of the crucible and raw material.

### Acknowledgments

The authors express their gratitude to A. Kajikura from Fujikoshi Machinery Corp. and Dr. T. Taishi from Shinshu University for their helpful and stimulating discussions. Part of this work was supported by “The research and development project for innovation technique of energy conservation” of the New Energy and Industrial Technology Development Organization (NEDO), Japan.

### References

- [1] H. H. Tappin, Optical Absorption and Photoconductivity in the Band Edge of β-Ga<sub>2</sub>O<sub>3</sub>, *Phys. Rev.*, **140** No.1A (1965) A316-A319.
- [2] M. Orita, H. Ohta, M. Hirano, and H. Hosono, Deep-ultraviolet transparent conductive β-Ga<sub>2</sub>O<sub>3</sub> thin films, *Appl. Phys. Lett.*, **77** No.25 (2000) 4166-4168.
- [3] M. Higashiwaki, K. Sasaki, A. Kuramata, T. Masui, and S. Yamakoshi, Gallium oxide (Ga<sub>2</sub>O<sub>3</sub>) metal-semiconductor field-effect transistors on single-crystal β-Ga<sub>2</sub>O<sub>3</sub> (010) substrates, *Appl. Phys. Lett.*, **100** (2012) 013504.
- [4] M. Higashiwaki, K. Sasaki, A. Kuramata, T. Masui, and S. Yamakoshi, Development of gallium oxide power devices, *Phys. Status Solidi A*, **211** No.1 (2014) 21-26.
- [5] T. Oishi, Y. Koga, K. Harada, and M. Kasu, High-mobility β-Ga<sub>2</sub>O<sub>3</sub>(-201) single crystals grown by edge-defined film-fed growth method and their Schottky barrier diodes with Ni contact, *Appl. Phys. Express*, **8** (2015) 031101.
- [6] Michele Baldini, Zbigniew Galazka, and Günter Wagner, Recent progress in the



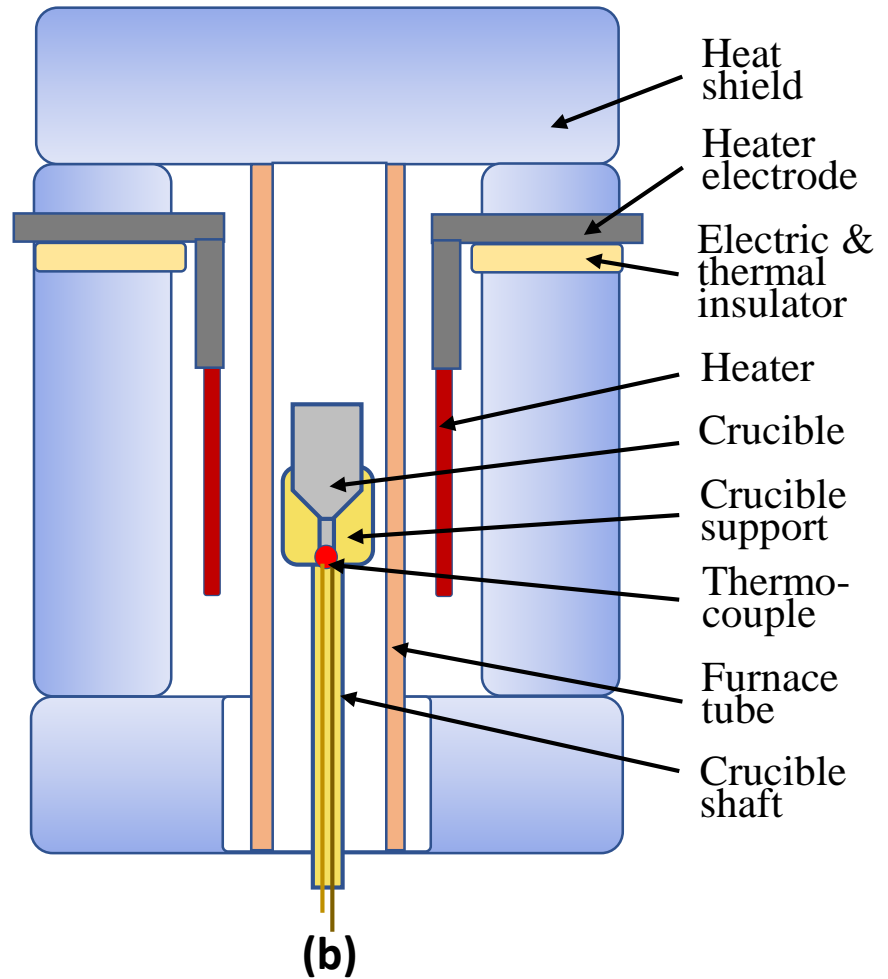
- growth of  $\beta$ -Ga<sub>2</sub>O<sub>3</sub> for power electronics applications, *Materials Science in Semiconductor Processing*, **78** (2018) 132-146.
- [7] N. Ueda, H. Hosono, R. Waseda, and H. Kawazoe, Synthesis and control of conductivity of ultraviolet transmitting  $\beta$ -Ga<sub>2</sub>O<sub>3</sub> single crystals, *Appl. Phys. Lett.*, **70** (26) (1997) 3561-3563.
- [8] E. G. Vllora, K. Shimamura, Y. Yoshikawa, K. Aoki and N. Ichinose, Large-size  $\beta$ -Ga<sub>2</sub>O<sub>3</sub> single crystals and wafers, *J. Cryst. Growth*, **270** (2004) 420–426.
- [9] E. G. Vllora, K. Shimamura, Y. Yoshikawa, T. Ujiie and K. Aoki, Electrical conductivity and carrier concentration control in  $\beta$ -Ga<sub>2</sub>O<sub>3</sub> by Si doping, *Appl. Phys. Lett.*, **92** (2008) 202120.
- [10] Y. Tomm, P. Reiche, D. Klimm, and T. Fukuda, Czochralski grown Ga<sub>2</sub>O<sub>3</sub> crystals, *J. Cryst. Growth*, **220** (2000) 510-514
- [11] Z. Galazka, R. Uecker, K. Irmscher, M. Albrecht, D. Klimm, M. Pietsch, M. Brutzam, R. Bertram, S. Ganschow, and R. Fornari, Czochralski growth and characterization of  $\beta$ -Ga<sub>2</sub>O<sub>3</sub> single crystals, *Cryst. Res. Technol.*, **45** No.12 (2010) 1229-1236.
- [12] Z. Galazka, K. Irmscher, R. Uecker, R. Bertram, M. Pietsch, A. Kwasniewski, M. Naumann, T. Schulz, R. Schewski, D. Klimm, and M. Bickermann, On the bulk  $\beta$ -Ga<sub>2</sub>O<sub>3</sub> single crystals grown by the Czochralski method, *J. Cryst. Growth*, **404** (2014) 184–191.
- [13] E. G. Vllora, S. Arjoca, K. Shimamura, D. Inomata, and K. Aoki,  $\beta$ -Ga<sub>2</sub>O<sub>3</sub> and single-crystal phosphors for high-brightness white LEDs & LDs, and  $\beta$ -Ga<sub>2</sub>O<sub>3</sub> potential for next generation of power devices, *Proc. of SPIE*, **8987** (2014) 89871U.
- [14] H. Aida, K. Nishiguchi, H. Takeda, N. Aota, K. Sunakawa, and Y. Yaguchi, Growth of  $\beta$ -Ga<sub>2</sub>O<sub>3</sub> Single Crystals by the Edge-Defined, Film Fed Growth Method, *Jpn. J. Appl. Phys.*, **47** No.11 (2008) 8506–8509.
- [15] E. G. Vllora, Y. Morioka, T. Atou, T. Sugawara, M. Kikuchi, and T. Fukuda, Infrared Reflectance and Electrical Conductivity of  $\beta$ -Ga<sub>2</sub>O<sub>3</sub>, *Phys. Stat. Sol. (a)*, **193** No.1 (2002) 187-195.
- [16] M. Zinkevich and F. Aldinger, Thermodynamic Assessment of the Gallium-Oxygen System, *J. Am. Ceram. Soc.*, **87** [4] (2004) 683–691.
- [17] D. Klimm, S. Ganschow, D. Schulz, R. Bertram, R. Uecker, P. Reiche, and R. Fornari, Growth of oxide compounds under dynamic atmosphere composition, *J. Cryst. Growth*, **311** (2009) 534–536.
- [18] K. Hoshikawa, H. Nakanishi, H. Kohda, and M. Sasaura, LIQUID ENCAPSULATED,

VERTICAL BRIDGMAN GROWTH OF LARGE DIAMETER, LOW DISLOCATION DENSITY, SEMI-INSULATING GaAs, *J. Cryst. Growth*, **94** (1989) 643-650.

- [19] C. Miyagawa, T. Kobayashi, T. Taishi, and K. Hoshikawa, Demonstration of crack-free c-axis sapphire crystal growth using the vertical Bridgman method, *J. Cryst. Growth*, **372** (2013) 95-99.
- [20] K. Hoshikawa, J. Osada, Y. Saitou, E. Ohba, C. Miyagawa, T. Kobayashi, J. Yanagisawa, M. Shinozuka, and K. Kanno, Vertical Bridgman growth of sapphire - Seed crystal shapes and seeding characteristics, *J. Cryst. Growth*, **395** (2014) 80-89.
- [21] K. Hoshikawa, E. Ohba, T. Kobayashi, J. Yanagisawa, C. Miyagawa, and Y. Nakamura, Growth of  $\beta$ -Ga<sub>2</sub>O<sub>3</sub> single crystals using vertical Bridgman method in ambient air, *J. Cryst. Growth* **447** (2016) 36-41.
- [22] E. Ohba, T. Kobayashi, M. Kado, and K. Hoshikwa, Defect characterization of  $\beta$ -Ga<sub>2</sub>O<sub>3</sub> single crystals grown by vertical Bridgman method, *Jpn. J. Appl. Phys.*, **55** (2016) 1202BF.



(a)



(b)

Fig. 1 Photograph (a) and schematic (b) of VB furnace

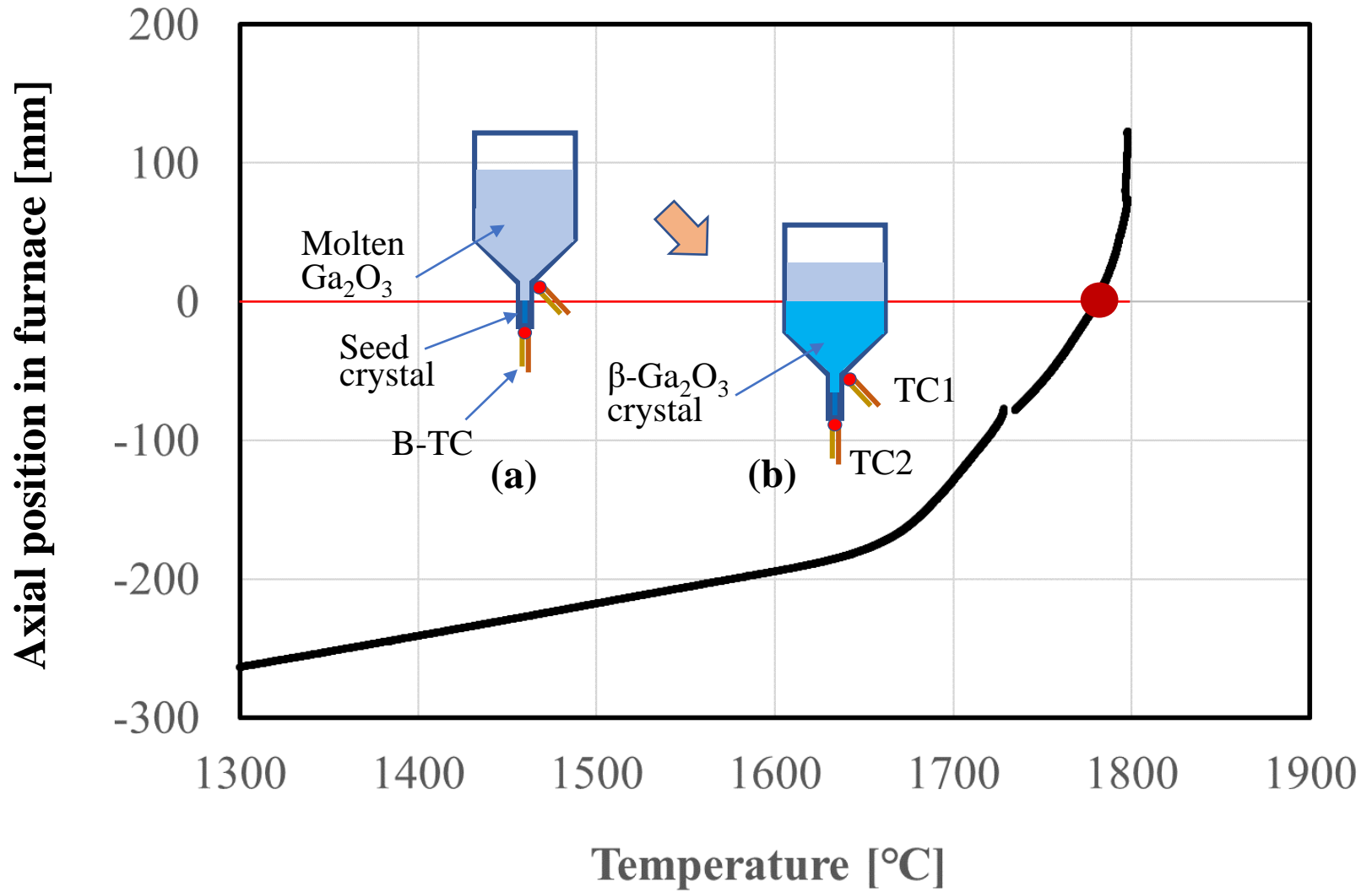


Fig. 2 Temperature distribution of VB furnace and schematics of VB growth processes

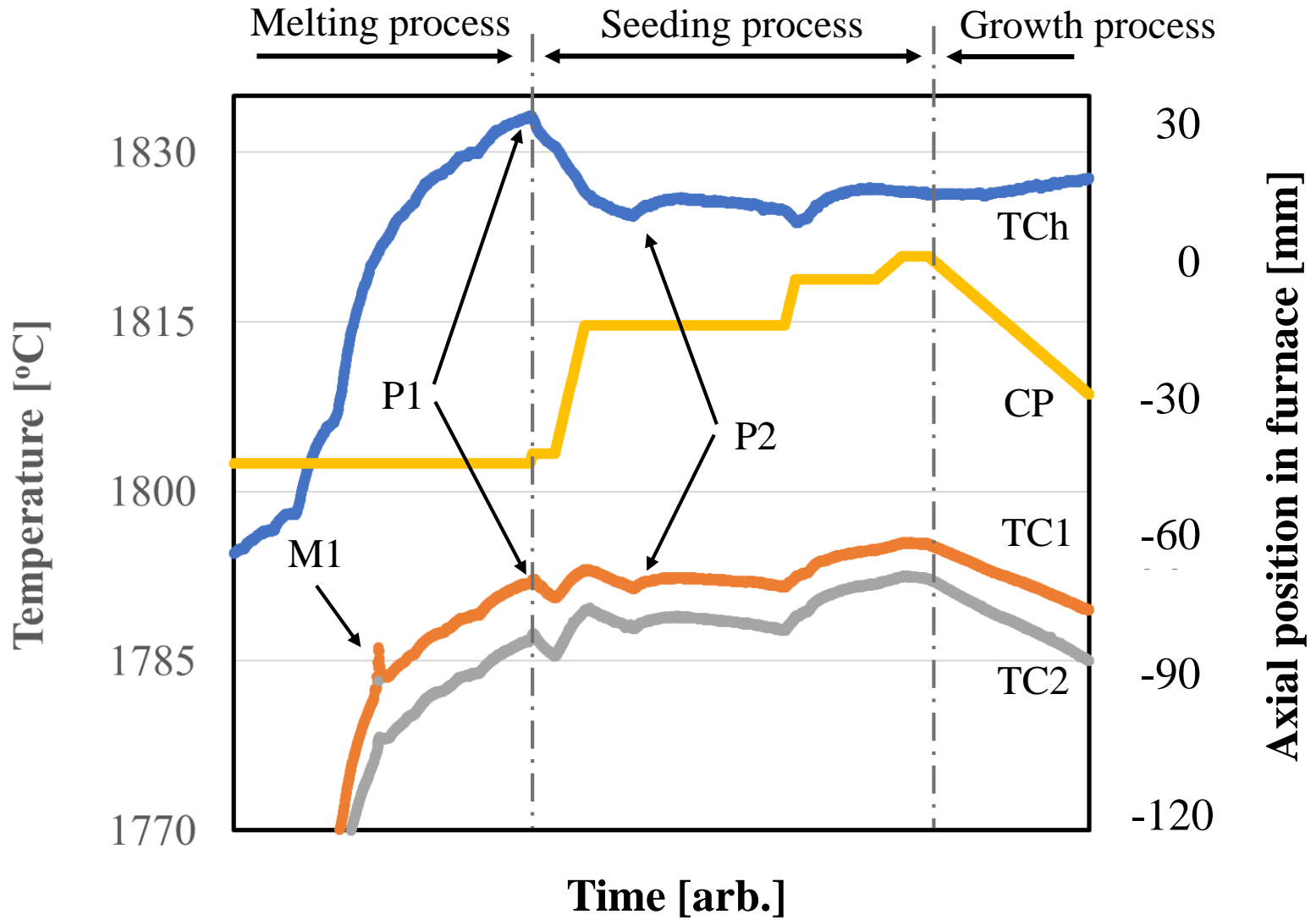


Fig. 3 Logger data of  $\beta$ -Ga<sub>2</sub>O<sub>3</sub> crystal growth by the VB process

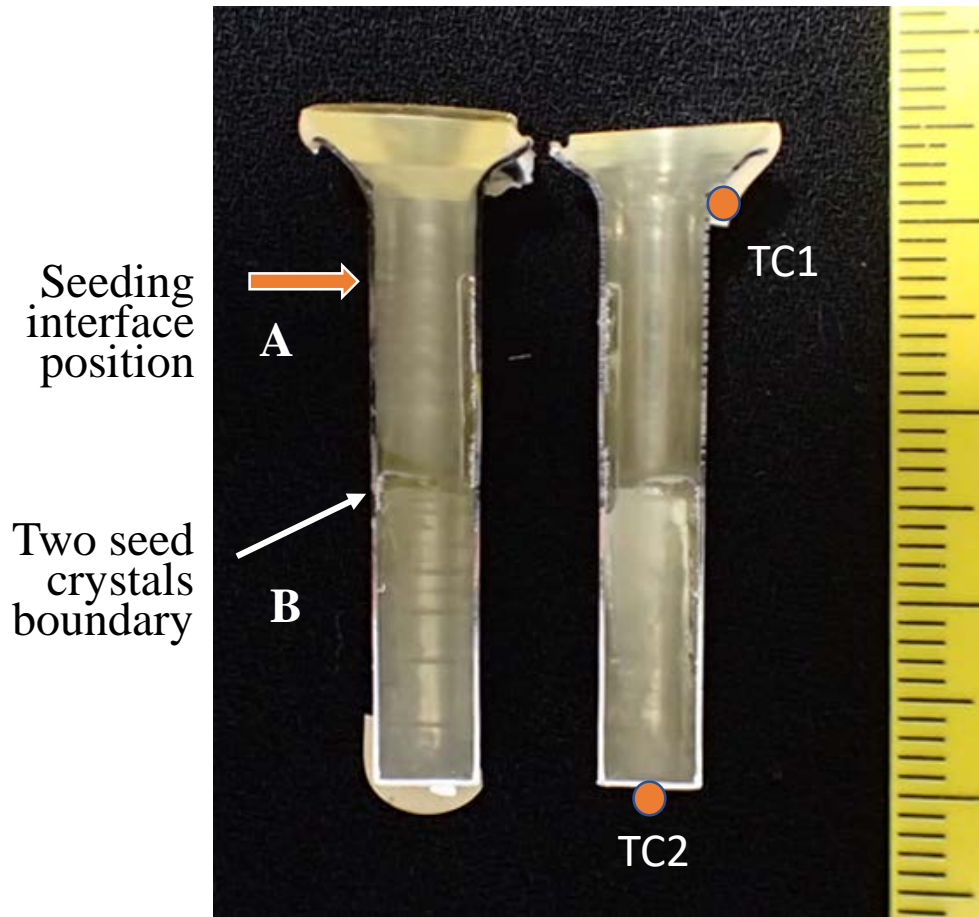


Fig. 4 Observation of seeding interface position

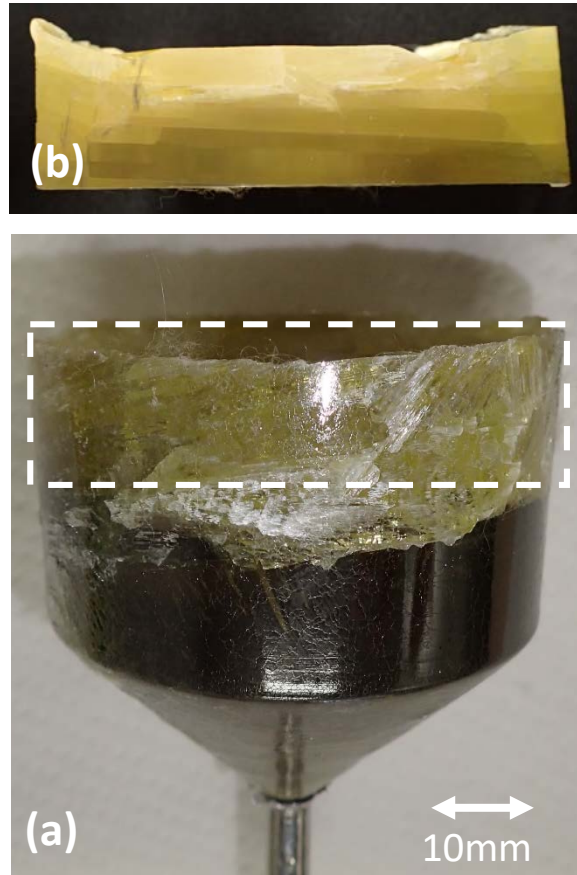


Fig. 5 Analysis of polycrystallization in growth orientation perpendicular to (100) plane.

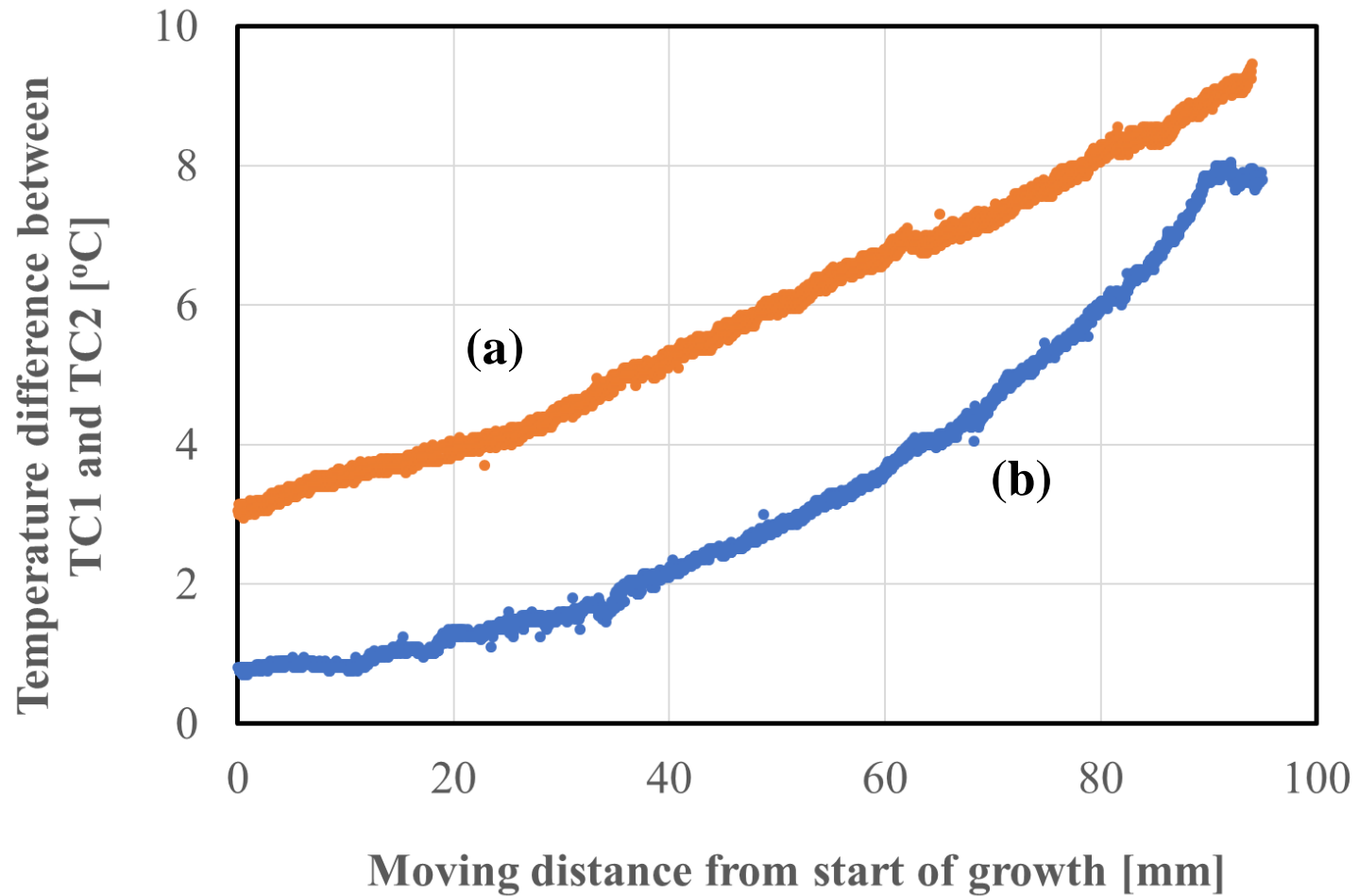


Fig. 6 Temperature difference  $\Delta T$  between TC1 and TC2 vs. moving distance from position at growth start.



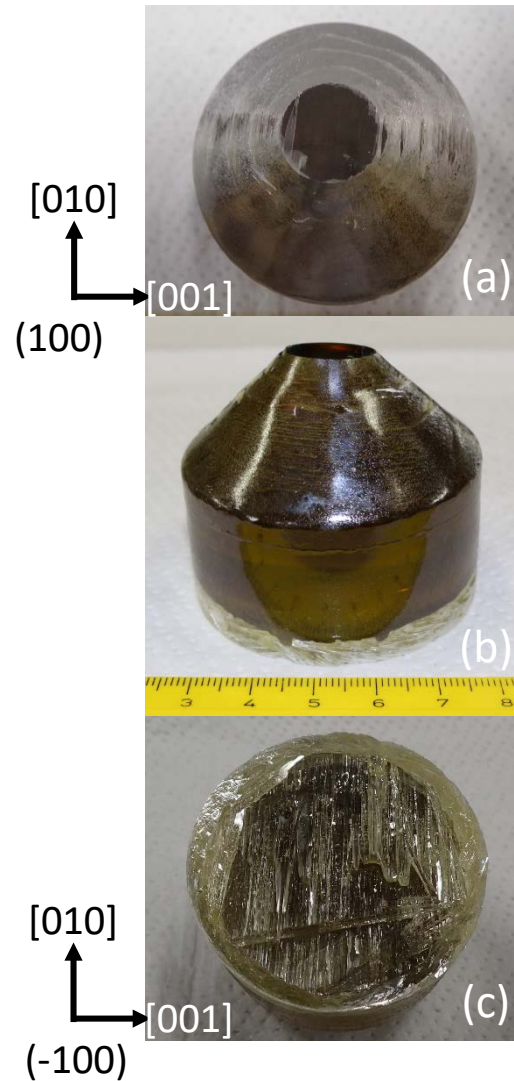


Fig. 7 2-inch diameter  $\beta$ - $\text{Ga}_2\text{O}_3$  single crystal with growth orientation perpendicular to  $(100)$  plane.

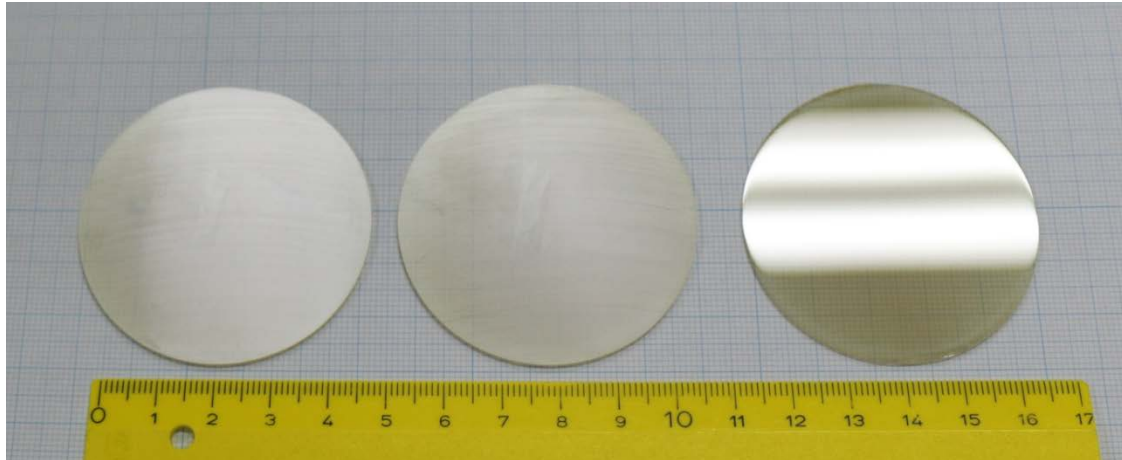


Fig. 8 Photographs of as-sliced wafers and mirror-polished wafer with (100) plane

Table 1 Weight losses of raw material Ga<sub>2</sub>O<sub>3</sub> during growth process

Run number of crystal growth	Total weight of raw material and crucible (g)	Retention time at more than 1770°C (h)	Total weight loss (g)
1	499	96	3.6
2	512	81	2.3
3	491	102	4.1

Table 2 Results of impurity analysis.

Element	Analysis result [wt.ppm]	
	g=0.5	g=0.9
Na	0.02	0.04
Mg	0.01	0.02
Al	0.44	0.41
Si	2.0	2.3
Ca	0.19	0.52
Fe	1.3	2.3
Zr	1.0	2.1
Sn	0.20	0.50
Pt	0.03	0.02
Rh	29	32